ELSEVIER

Biochimica et Biophysica Acta 1285 (1996) 101–108

BIOCHIMICA ET BIOPHYSICA ACTA
BBA

Metastable rippled gel phase in saturated phosphatidylcholines: calorimetric and densitometric characterization

Rumiana Koynova *, Assen Koumanov, Boris Tenchov

Institute of Biophysics, Bulgarian Academy of Sciences, 1113 Sofia, Bulgaria

Received 23 April 1996; revised 9 July 1996; accepted 11 July 1996

Abstract

A long-living metastable rippled phase $P_{\beta'}^{mst}$ has been earlier reported to form in aqueous dispersions of dipalmitoylphosphatidylcholine (DPPC) upon cooling from the lamellar liquid crystalline phase L_α (Tenchov et al. (1989) Biophys. J. 56, 757–768). Here we demonstrate that similar metastable phases form also in distearoylphosphatidylcholine (DSPC) and dihexadecylphosphatidylcholine (DHPC) but not in dimyristoylphosphatidylcholine (DMPC). The thermodynamic parameters of $P_{\beta'}^{mst}$ in DPPC, DSPC and DHPC have been characterized in detail by means of differential scanning calorimetry and scanning densitometry. It is shown that the $P_{\beta'}^{mst}$ phase in these three lipids has higher specific heat capacity by 0.1–0.4 kcal K^{-1} mol^{-1} and higher specific volume by 1–2 $\mu l/g$ than the equilibrium $P_{\beta'}$ phase formed upon heating from the $L_{\beta'}$ phase. The $P_{\beta'}^{mst} \rightarrow L_\alpha$ transition in these three lipids takes place at 0.06–0.14°C lower temperature than the $P_{\beta'} \rightarrow L_\alpha$ transition. Its enthalpy is lower by 5–11% and the apparent maximum specific heat C_p^{max} is lower by 11–14%. The $P_{\beta'}^{mst}$ phase is a long-living phase – it does not relax into the equilibrium $P_{\beta'}$ for at least several hours. The replacement of the ester glycerol-hydrocarbon chain linkages in DPPC with ether bonds in DHPC does not influence the formation of $P_{\beta'}^{mst}$.

Keywords: Phase transition; Phospholipid; Polymorphism; Membrane; Scanning densitometry; DSC

1. Introduction

Aqueous dispersions of dipalmitoylphosphatidylcholine (DPPC) are known to form lamellar liquid-crystalline (L_α) phase at high temperature, two lamellar gel phases ($L_{\beta'}$ and $P_{\beta'}$) at intermediate temperatures, and lamellar subgel (L_c) phase at low temperature [1]. Recent investigations report for two additional metastable phases forming in it. One of these phases is an ordered subgel phase (SGII) forming reversibly at low temperature (< 7°C), a precursor of the equilibrium crystalline L_c phase [2,3]. Further, the formation of SGII was observed to take place also in other saturated PC-water systems [3]. Another metastable phase, $P_{\beta'}^{mst}$, has been reported to form in DPPC upon cooling from the L_α phase [4–6]. It replaces the equilibrium $P_{\beta'}$ phase which forms upon heating from the $L_{\beta'}$ phase. The metastable $P_{\beta'}^{mst}$ phase is long living in the temperature range between the pretransition and the main transition but readily converts to the initial $P_{\beta'}$ phase upon cooling to the $L_{\beta'}$ phase and subsequent reheating through the pretransition. High-resolution X-ray scattering data

Abbreviations: DPPC, 1,2-dipalmitoyl-*sn*-glycero-3-phosphocholine; DMPC, 1,2-dimyristoyl-*sn*-glycero-3-phosphocholine; DSPC, 1,2-distearoyl-*sn*-glycero-3-phosphocholine; DHPC, 1,2-dihexadecyl-*sn*-glycero-3-phosphocholine.

* Corresponding author. Fax: +359 2 9712493; e-mail: rkoynova@bgearn.bitnet, koynova@boi.acad.bg.

PII S0005-2736(96)00155-1

demonstrate that two ripple structures form upon cooling from the L_α phase – a primary one coinciding with that of the 'normal' $P_{\beta'}$ phase, with ripple wavelength of 13 nm, and a secondary one with doubled ripple wavelength of 26 nm [5,6]. Such ripple structures have been also observed earlier, using freeze-fracture electron microscopy [7]. In the present work, we used high-sensitivity differential scanning calorimetry and scanning densitometry for a detailed determination of the thermodynamic characteristics of the $P_{\beta'}^{mst}$ phase, and also in order to check for the formation of similar phases in other phosphatidylcholines of similar chemical structure and phase behavior, namely, DMPC and DSPC which differ from DPPC by ± 2 CH_2 groups in their hydrocarbon chains, and DHPC which differ from DPPC only by the glycerol-hydrocarbon chain linkage (ether instead of ester).

2. Materials and methods

2.1. Sample preparation

1,2-Dimyristoyl-*sn*-glycero-3-phosphocholine (DMPC), 1,2-dipalmitoyl-*sn*-glycero-3-phosphocholine (DPPC), 1,2-distearoyl-*sn*-glycero-3-phosphocholine (DSPC) (Avanti Polar Lipids, Birmingham, AL) and 1,2-dihexadecyl-*sn*-glycero-3-phosphocholine (DHPC) (Fluka, Basel) were used. No chromatographic tests for purity were performed, however, the half-widths of the main phase transitions (ca. 0.20–0.25 K) provided a guarantee that the lipid purities were comparable with the claimed value of $> 99\%$.

Multilamellar lipid vesicles were prepared by dispersing lipid in required amounts of quartz-bidistilled deionized water. The dispersions were hydrated overnight at 20°C and cycled 5–10-times between a temperature 10 K above the main transition and ice bath. The samples were vortex-mixed at these temperatures for 1–2 min. The lipid concentrations were 0.3–0.6 mg/ml for calorimetry and 10 mg/ml for densitometry.

2.2. Calorimetric measurements

Calorimetric measurements were performed using high-sensitivity differential adiabatic scanning microcalorimeters DASM-1M and DASM-4 (Biopribor, Pushchino, Russia) with sensitivity better than $4 \cdot 10^{-6}$ cal K^{-1} and a noise level less than $5 \cdot 10^{-7}$ W [8]. Heating runs were performed with a scan rate of 0.5 K/min. The temperature at the maximum of the excess heat capacity curve was taken as the transition temperature T_m and the transition width $\Delta T_{1/2}$ was determined at the transition half-height. The specific heat capacity of the lipid $C_p^{lip}(T)$ was calculated using the relationship [9]:

$$C_p^{lip}(T) = \frac{C_{p,app}^{H_2O}(T)}{V_{app}^{H_2O}(T)} V_{app}^{lip}(T) - \frac{\Delta C_{p,obs}(T)}{m_{lip}}$$

Here $C_{p,app}^{H_2O}(T)$ and $V_{app}^{H_2O}(T)$ are the apparent specific heat capacity and volume of water taken from Handbook of Chemistry and Physics, 66th Edn. (1985-86) [10], $\Delta C_{p,obs}(T)$ is the observed difference in heat capacity between the lipid dispersion and the water baseline, $V_{app}^{lip}(T)$ is the apparent specific volume of lipid as determined by densitometric measurements (see below), and m_{lip} is the mass of the lipid. The calorimetric enthalpy ΔH^{cal} of the transition was determined as the area under the excess heat capacity curve. The van't Hoff enthalpy ΔH^{vH} was calculated from the calorimetric data by using the relationship [11]:

$$\Delta H^{vH} = 4RT^2 C_p^{max} / \Delta H^{cal}$$

where C_p^{max} is the maximum excess heat capacity.

2.3. Densitometric measurements

The specific volume of the lipid molecules in the different phases was calculated from the density difference between water and the lipid dispersions. The latter was determined by using two DMA-602H cells (Anton Paar, Graz) connected to a home-made unit for data acquisition and temperature control. Linear heating and cooling of the samples was performed at scan rates between 0.1 and 1 K/min with a Heto water bath (Heto Lab Equipment, Allerod, Denmark). The instrument constants were determined according to the specifications of the producer, using distilled water and air as standards. The densities of air and water as a function of temperature were taken from the Handbook of Chemistry and Physics, 66th Edn.

(1985-86). The partial specific volume of lipids was calculated according to the equation [12]:

$$\bar{v} = \frac{1}{\rho_{H_2O}}\left(1 - \frac{\rho_{lip} - \rho_{H_2O}}{c}\right)$$

where ρ_{lip} and ρ_{H_2O} are the densities of the solution and solvent (water), respectively, and c is the lipid concentration. No concentration dependence of the apparent specific volume of lipids was observed in the employed concentration range.

3. Results and discussion

3.1. Differential scanning calorimetry

All four lipids, DMPC, DPPC, DSPC, and DHPC, are known to undergo $P_{\beta'} \rightarrow L_{\alpha}$ transition upon melting [1]. The diacyl species DMPC, DPPC and DSPC undergo an $L_{\beta'} \rightarrow P_{\beta'}$ transformation during the pretransition, while in the dialkyl lipid DHPC the gel phase below the pretransition is interdigitated [13]. Following cooling form the L_{α} phase, two types of heating scans were performed with these lipids: starting from temperature more than 10°C below the pretransition ('$L_{\beta'}$ scan'), or starting from temperature in the range between the pretransition and the main transition ('$P_{\beta'}$ scan'). Since the studied differences in the thermodynamic parameters are expectedly small [4], and as it is known that the major source of error stems from filling the inhomogeneous lipid dispersions into the calorimetric cell [14,15], series of at least 20 heating scans were performed with the same sample in the calorimetric cell. In some cases, the sample was incubated for some time (30 min – 4 h) at the initial temperature before starting the measurement. Scans of the two types were randomly alternated. We did not observe systematic dependence of the thermodynamic behavior of the sample on the temperature prehistory of the preceding heating scan, neither on the time of incubation or the particular temperature of incubation within the given temperature range. Representative scans of the two types, in two different Y-axis scales, for the four studied phosphatidylcholines, are shown in Figs. 1–4. The small shoulder preceding the main transition of DSPC (Fig. 3) possibly reflects the recently reported sub-main transition in long-chain phosphatidylcholines [17]. Thermodynamic parameters of the phase transitions (temperature T_{pre} and calorimetric enthalpy ΔH_{pre} of the pretransition, and temperature T_m, calorimetric enthalpy ΔH^{cal}, width at half-height $\Delta T_{1/2}$, apparent maximum heat capacity C_p^{max}, change in the specific heat capacity before and after the transition ΔC_p, and van't Hoff enthalpy ΔH^{vH} for the main transition) averaged over at least 10 heating scans, are presented in Table 1 (orientational temperature ranges for the scans of the two types in each case are indicated in brackets).

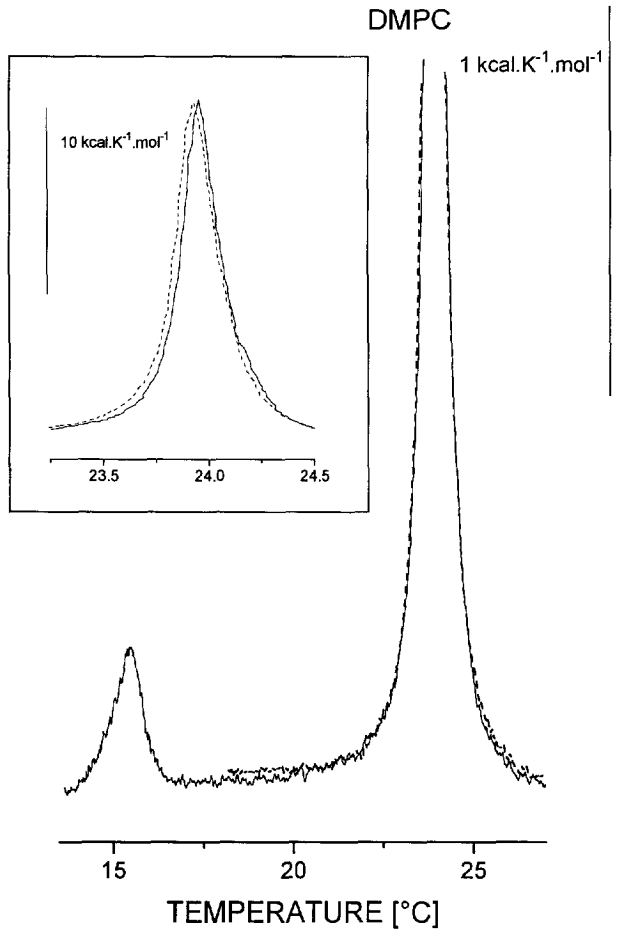

Fig. 1. DSC heating thermograms (in two different Y-scales) of hydrated DMPC dispersion recorded after cooling from 28°C to 10°C (full line) and to 17°C (dashed line). Heating rate 0.5 K/min.

Table 1
Thermodynamic parameters of the pretransition and main transition of saturated phosphatidylcholines during '$L_{\beta'}$ scan' and '$P_{\beta'}$ scan' (see text) as determined by differential scanning calorimetry

	T_{pre} (°C)	ΔH_{pre} (kcal/mol)	T_m (°C)	$\Delta T_{1/2}$ (K)	ΔH^{cal} (cal/mol)	C_p^{max} (cal/K/mol)	ΔC_p (cal/K/mol]	ΔH^{vH} (kcal/mol)
DMPC								
$L_{\beta'}$ scan (10–28°C)	14.63 ± 0.99	0.71 ± 0.14	23.94 ± 0.03	0.21 ± 0.02	6.04 ± 0.11	18.09 ± 0.27	−34.27 ± 32.33	2113 ± 63
$P_{\beta'}$ scan (16–28°C)			23.93 ± 0.01	0.22 ± 0.03	6.17 ± 0.21	18.00 ± 0.13	−51.64 ± 46.56	2057 ± 68
DPPC								
$L_{\beta'}$ scan (20–45°C)	35.51 ± 0.23	0.90 ± 0.19	41.47 ± 0.03	0.22 ± 0.02	7.96 ± 0.19	23.90 ± 0.46	−47.34 ± 21.26	2377 ± 107
$P_{\beta'}$ scan (35–45°C)			41.41 ± 0.02	0.28 ± 0.01	7.55 ± 0.18	20.85 ± 0.24	−130.67 ± 15.74	2128 ± 86
DSPC								
$L_{\beta'}$ scan (30–58°C)	50.87 ± 0.40	0.98 ± 0.08	54.78 ± 0.04	0.27 ± 0.03	11.25 ± 0.57	30.48 ± 0.58	−61.61 ± 28.87	2330 ± 20
$P_{\beta'}$ scan (52–58°C)			54.64 ± 0.04	0.27 ± 0.03	10.02 ± 0.39	26.05 ± 0.67	−465.53 ± 122.27	2232 ± 75
DHPC								
$L_{\beta'}$ scan (20–48°C)	34.70 ± 0.07	1.81 ± 0.58	44.09 ± 0.02	0.30 ± 0.03	9.61 ± 0.49	26.90 ± 0.47	−68.34 ± 21.59	2252 ± 77
$P_{\beta'}$ scan (35–48°C)			44.03 ± 0.03	0.30 ± 0.02	9.14 ± 0.62	23.90 ± 0.84	−173.71 ± 24.42	2103 ± 87

Orientational temperature ranges of the '$L_{\beta'}$ scan' and '$P_{\beta'}$ scan' are given in brackets.

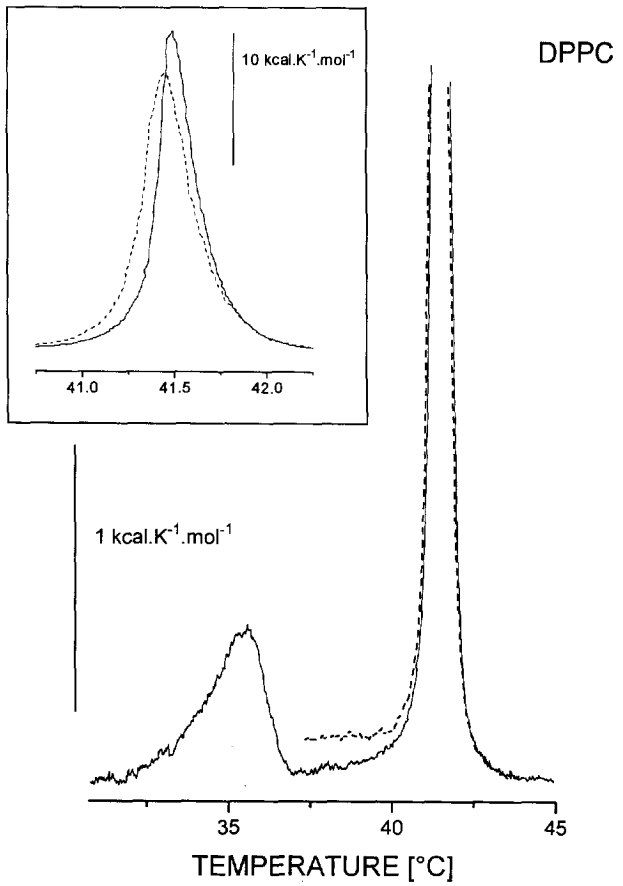

Fig. 2. DSC heating thermograms (in two different *Y*-scales) of hydrated DPPC dispersion recorded after cooling from 45°C to 20°C (full line) and to 35°C (dashed line). Heating rate 0.5 K/min.

The obtained data could be summarized as follows:

– For DSPC, DPPC and DHPC, the temperature of the main transition during a '$P_{\beta'}$ scan' is lower as compared to '$L_{\beta'}$ scan'. This difference is 0.06 K for DPPC and DHPC, and 0.14 K for DSPC. For DMPC the main transition temperature is the same for the two types of scans.

– The apparent maximum heat capacity C_p^{max} of the main transition is lower by 3 kcal K^{-1} mol^{-1} for DPPC and DHPC and by 4.4 kcal K^{-1} mol^{-1} for DSPC during a '$P_{\beta'}$ scan' than during an '$L_{\beta'}$ scan'. For DMPC, no confident difference in C_p^{max} is observed.

– The calorimetric enthalpy ΔH^{cal} of the main transition is lower during a '$P_{\beta'}$ scan' than during an '$L_{\beta'}$ scan' for DSPC, DPPC and DHPC by 1.2, 0.4 and 0.5 kcal mol^{-1}, respectively, while for DMPC the two enthalpies coincide within the error limits.

– Incubations for periods of 30 min to 4 h in the temperature range between the pretransition and the main transition did not eliminate the registered differences in the two types of scans.

With account to these data we conclude that long-living metastable ripple phases $P_{\beta'}^{mst}$ similar in their thermodynamic manifestation to that observed previously in DPPC upon cooling from L_α phase, form also in DSPC and DHPC, but not in DMPC. For DMPC either such phase is short-living, or rather, the equilibrium rippled phase $P_{\beta'}$ is immediately formed.

For the studied lipids we observed a small negative change of the specific heat capacity (ΔC_p) after the

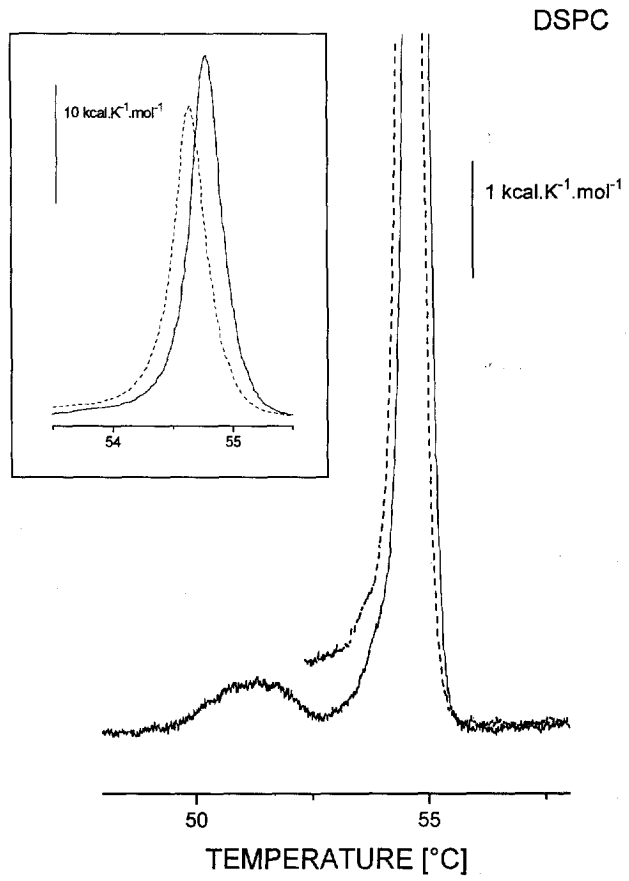

Fig. 3. DSC heating thermograms (in two different *Y*-scales) of hydrated DSPC dispersion recorded after cooling from 58°C to 30°C (full line) and to 51°C (dashed line). Heating rate 0.5 K/min.

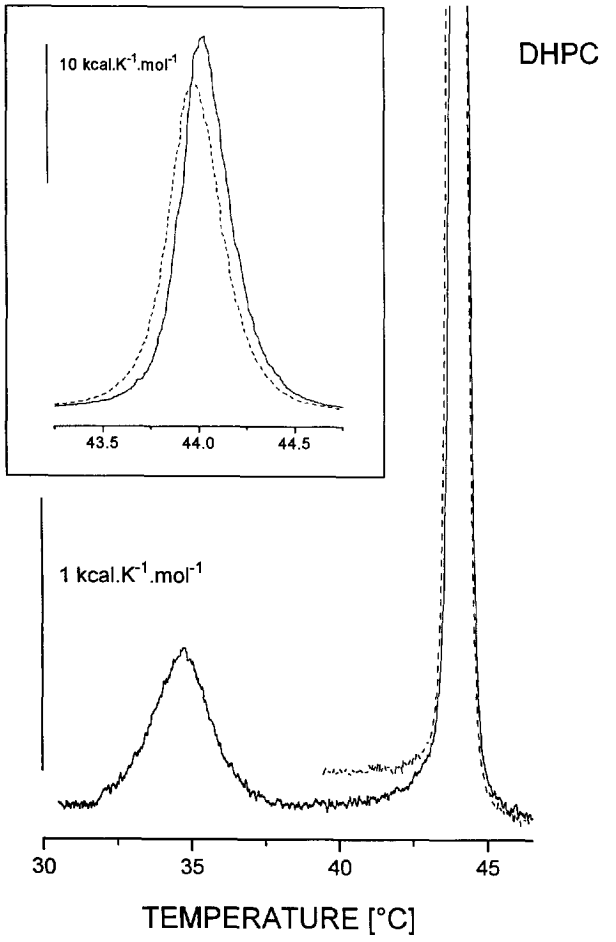

Fig. 4. DSC heating thermograms (in two different *Y*-scales) of hydrated DHPC dispersion recorded after cooling from 48°C to 20°C (full line) and to 38°C (dashed line). Heating rate 0.5 K/min.

main transition for both '$P_{\beta'}$ scan' and '$L_{\beta'}$ scan', i.e., the L_α phase has lower specific heat capacity than the phases preceding the transition. A higher baseline position for the $P_{\beta'}$ phase between the $L_{\beta'}$ and L_α phases in diacylphosphatidylcholines has been previously noticed [14–16]. Potential reason is a partial overlapping of the pre- and main transition. Indeed, increasing the lipid concentration above 1 mg/ml results in a progressive upward shift of the baseline between the two transitions. Decrease of the lipid concentration below the values employed in the present study, however, did not result in a change of the baseline position. Thus, it seems that the $P_{\beta'}$ phase is characterized indeed by slightly higher specific heat (by 35–70 cal K^{-1} mol^{-1}) than the L_α phase. Further, we observe an enhanced negative change of the specific heat during a $P_{\beta'}^{mst} \rightarrow L_\alpha$ transition for DPPC, DSPC and DHPC as compared to the $P_{\beta'} \rightarrow L_\alpha$ transition. This effect is apparently due to a higher specific heat of the $P_{\beta'}^{mst}$ in comparison to the equilibrium $P_{\beta'}$ phase, since the specific heat of the L_α phase remains unchanged. According to the data in Table 1, the specific heat capacity of the $P_{\beta'}^{mst}$ exceeds that of the $P_{\beta'}$ phase by ca. 80, 100 and 400 cal K^{-1} mol^{-1} for DPPC, DHPC and DSPC, respectively. Incubation for up to 4 h in the temperature range between the pretransition and the main transition did not merge the excess specific heats of the two phases.

3.2. Scanning densitometry

For all four studied lipids the specific volume as a function of temperature was determined during heating and cooling scans with scan rates 0.1–1 K/min. Collection of representative scans is presented on Fig. 5. The specific volumes at temperatures in the range between the pretransition and the main transition, as well as the volume change during the main transition as measured from these scans are summarized in Table 2. As seen from the presented data, the specific volume of DPPC, DSPC, and DHPC in the temperature range between the pre- and main transition dur-

Table 2
Specific volumes *V* of the phases between pretransition and main transition ($P_{\beta'}$ upon heating and $P_{\beta'}^{mst}$ upon cooling) and volume changes ΔV during the main transition for saturated phosphatidylcholines

	$V(P_{\beta'}/P_{\beta'}^{mst})$ (ml/g)	ΔV (ml/g)
DMPC		
Heating	0.9402 (22°C)	0.0254
Cooling	0.9403 (22°C)	0.0253
DPPC		
Heating	0.9550 (37.5°C)	0.0424
Cooling	0.9561 (37.5°C)	0.0412
DSPC		
Heating	0.9754 (51°C)	0.0505
Cooling	0.9776 (51°C)	0.0481
DHPC		
Heating	0.9882 (37.5°C)	0.0394
Cooling	0.9902 (37.5°C)	0.0367

The temperatures to which the specific volume values refer are given in brackets.

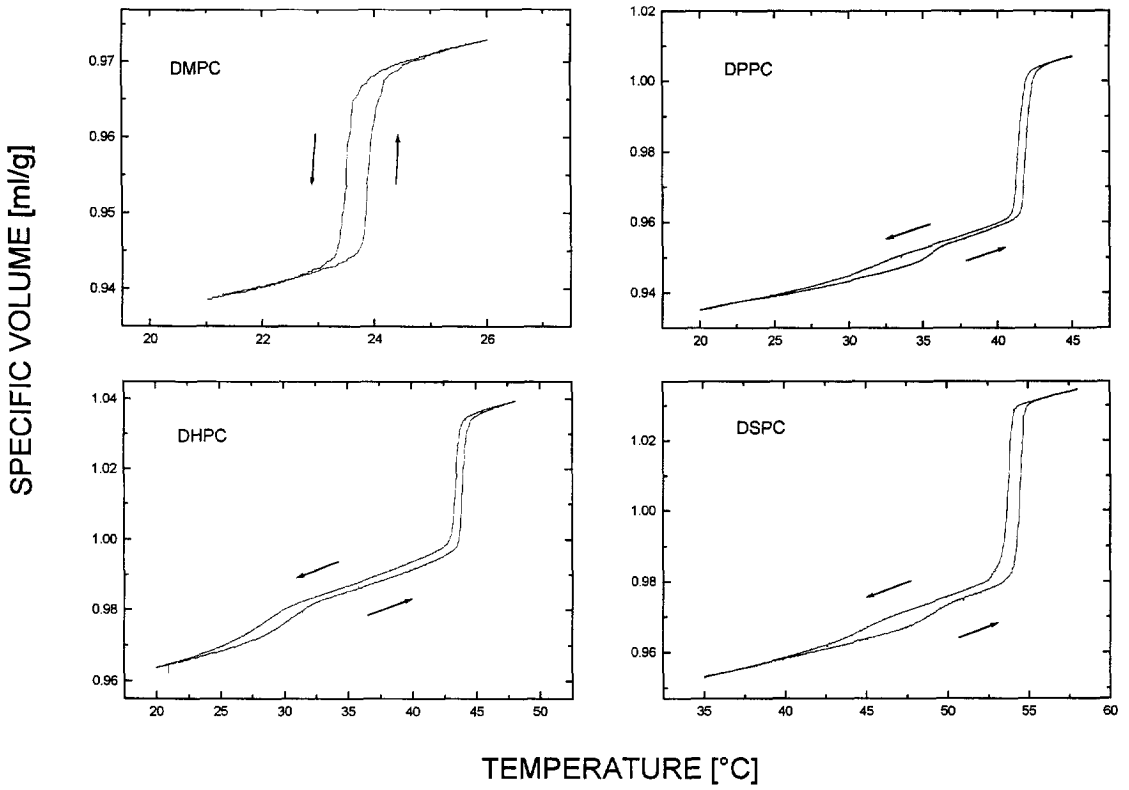

Fig. 5. Densitometric heating and cooling traces of hydrated DMPC, DPPC, DSPC, and DHPC dispersions recorded at a scan rate of 0.5 K/min.

ing cooling scans is higher by 1–2 μl/g in comparison to that during the heating scans. Correspondingly, the volume changes during the main transition is by 3–7% lower upon cooling scans for these three lipids as compared to the heating scans. For DMPC, the specific volumes in the two cases coincide and the volume changes in both directions are practically the same. These data confirm the calorimetric data illustrating the formation of a metastable rippled phase in DPPC, DSPC and DHPC but not in DMPC.

Noteworthy, the difference in the specific volumes between the $P_{\beta'}$ and $P_{\beta'}^{mst}$ phases does not depend on the scan rate. On Fig. 6, the specific volume as a function of temperature for DPPC suspension as recorded at 0.1 and 1 K/min is plotted. As seen from the figure, only the temperature hysteresis of the main transition but not the specific volumes of the $P_{\beta'}$ and $P_{\beta'}^{mst}$ phases change upon such change in the scan rate.

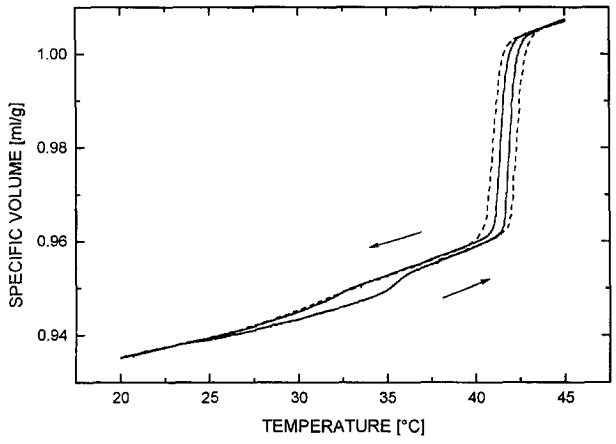

Fig. 6. Densitometric heating and cooling traces of hydrated DPPC dispersion recorded at scan rate of 0.1 K/min (full line) and 1 K/min (dashed line).

4. Conclusions

Metastable rippled phases $P_{\beta'}^{mst}$ similar in their thermodynamic manifestation to that in DPPC, form also in DSPC and DHPC, but not in DMPC. Using high-sensitivity DSC and scanning densitometry, we characterise in detail the thermodynamic parameters of these phases. The $P_{\beta'}^{mst}$ phase has by 0.1–0.4 kcal K^{-1} mol^{-1} higher specific heat capacity and by 1–2 $\mu l/g$ higher specific volume than the equilibrium $P_{\beta'}$ phase formed upon heating from the $L_{\beta'}$ phase in the three lipids. For DMPC, the phases formed during the cooling from the L_α phase and during heating from the $L_{\beta'}$ phase are indistinguishable with respect to their specific heat capacity and volume. Also, the $P_{\beta'}^{mst} \rightarrow L_\alpha$ transition takes place at 0.06–0.14°C lower temperature and with 11–14% lower apparent maximum heat capacity C_p^{max} than the $P_{\beta'} \rightarrow L_\alpha$ transition in DPPC, DSPC and DHPC. The $P_{\beta'}^{mst}$ phase is a long living one – it does not relax into the $P_{\beta'}$ phase for at least several hours. Thus, formation of metastable rippled phase in saturated diacylphosphatidylcholines is favorable for chain length of 16 and more carbon atoms. The replacement of the ester glycerol-chain linkages with ether ones does not prevent the formation of $P_{\beta'}^{mst}$ phase.

Acknowledgements

Financial support from grant K-407/1994 of the Bulgarian National Science Foundation is gratefully acknowledged.

References

[1] NIST Standard Reference Database 34 (1994) Lipid Thermotropic Phase Transition Database (LIPIDAT), Version 2.0.
[2] Slater, J.L. and Huang, C. (1987) Biophys. J. 52, 667–670.
[3] Koynova, R., Tenchov, B.G., Todinova, S. and Quinn, P.J. (1995) Biophys. J. 68, 2370–2375.
[4] Tenchov, B.G., Yao, H. and Hatta, I. (1989) Biophys. J. 56, 757–768.
[5] Yao, H., Matuoka, S., Tenchov, B. and Hatta, I. (1991) Biophys. J. 59, 252–255.
[6] Matuoka, S., Yao, H., Kato, S. and Hatta, I. (1993) Biophys. J. 64, 1456–1460.
[7] Copeland, B.R. and McConnell, H.M. (1980) Biochim. Biophys. Acta 599, 95–109.
[8] Privalov, P.L., Plotnikov, V.V. and Filimonov, V.V. (1975) J. Chem. Thermodyn. 7, 41–47.
[9] Privalov, P.L. and Potekhin, S.Y. (1986) Methods Enzymol. 131, 4–51.
[10] Weast, R.C. (ed.) (1985-86) CRC Handbook of Chemistry and Physics, 66th Edn., CRC Press, Boca Raton, FL.
[11] Jackson, W.M. and Brands, J.F. (1970) Biochemistry 9, 2294–2301.
[12] Kratky, O., Leopold, H. and Stabinger, H. (1973) Methods Enzymol. 27, 98–110.
[13] Laggner, P., Lohner, K., Degovics, G., Muller, K. and Schuster, A. (1987) Chem. Phys. Lipids 44, 31–60.
[14] Blume, A. (1983) Biochemistry 22, 5436–5442
[15] Wilkinson, D.A. and Nagle, J.F. (1982) Biochim. Biophys. Acta 688, 107–115.
[16] Hinz, H.-J. and Sturtevant, J.M. (1972) J. Biol. Chem. 247, 6071–6075.
[17] Jørgensen, K. (1995) Biochim. Biophys. Acta 1240, 111–114.